

Rice Husk Powder-Filled Polystyrene/Styrene Butadiene Rubber Blends

M. Zurina, H. Ismail, A. A. Bakar

School of Materials and Mineral Resources Engineering, Engineering Campus, Universiti Sains Malaysia, 14300 Nibong Tebal, Pulau Pinang, Malaysia

Received 14 May 2003; accepted 13 November 2003

ABSTRACT: Natural fibers are rich in cellulose and they are a cheap, easily renewable source of fibers with the potential for polymer reinforcement. The presence of large amounts of hydroxyl groups makes natural fibers less attractive for reinforcement of polymeric materials. Composites made from polystyrene (PS)/styrene butadiene rubber (SBR) blend and treated rice husk powder (RHP) were prepared. The RHP was treated by esterification and acetylation. A similar series of composites was also prepared using maleic anhydride-polypropylene (MA-PP) as a coupling agent. The processing behavior, mechanical properties, effect of thermooxidative ageing, and surface morphology of untreated and chemically modified RHP were studied. There was a decrease in tensile strength (except MA-PP composites), elongation at break, and Young's modulus in

chemically treated RHP composites. The postreaction process during thermooxidative ageing enhanced the tensile strength and Young's modulus of the esterified and MA-PP composites. Acetylation treatment was effective in reducing the percentage of water absorption in RHP/PS-SBR composites. In general chemically treated RHP/PS-SBR composites and MA-PP showed a better matrix phase and filler distribution. However, the degree of filler-matrix interaction was mainly responsible for the improvement of mechanical properties in the composites. © 2004 Wiley Periodicals, Inc. *J Appl Polym Sci* 92: 3320–3332, 2004

Key words: composites; blends; polystyrene; mechanical properties; natural fibers

INTRODUCTION

Rice husk powder (RHP) is a waste from agricultural activities and is abundant in Malaysia and neighboring countries. The present technique of disposing of this material is by open burning, which has now become an environmental issue because it contributes to air pollution. The use of RHP as a filler in polymer matrices has become one of the alternative methods for using this waste material and at the same time overcoming environmental problems.^{1,2}

It is well known that there are environmental and economical advantages to produce natural filler/thermoplastic elastomer composites. Cellulosic filler-reinforced plastics materials are low cost, lightweight, free from health hazards, have enhanced mechanical properties, and thus have the potential for structural application. Although their use is not as popular as that of mineral or inorganic fillers, use of natural fillers is appealing because of their renewable nature, low cost, low density, amenability to chemical modification, flexibility during processing with no harm to the equipment, and biodegradable nature, which may contribute to a healthy ecosystem.^{3,4}

Unfortunately, the high hydroxyl group content of cellulose is the main cause of poor compatibility between hydrophilic natural fillers and hydrophobic polymers used as matrix.⁵ Similar surface tension and similar polarity of matrix and fillers are required for good interfacial adhesion in natural filler-reinforced polymer composites. To produce reactive hydroxyl groups and a rough surface for adhesion with polymeric materials, plant fibers need to undergo physical and/or chemical treatment to modify the surface structure.⁶ The performance and stability of composite reinforced natural fillers depend on the development of strong interfacial bonding between fiber and matrix.

In this work, esterification, acetylation, and the use of maleic anhydride-polypropylene (MA-PP) were carried out with the aim of decreasing the natural hydrophilic character of rice husk powder as a filler and to study the performance of treated rice husk powder-filled polystyrene/styrene butadiene rubber (RHP/PS-SBR) composites.

EXPERIMENTAL

Materials

Polystyrene (PS; grade HH35) used in this study was from Petrochemical (M) Sdn. Bhd. (Johor, Malaysia), with a melt flow index (MFI) value of 5.8 g/10 min at

Correspondence to: H. Ismail (hanafi@eng.usm.my).

TABLE I
Composition of the Composite

Material (php) ^a	Composite				
	A	B	C	D	E
Polystyrene (PS)	80	80	80	80	80
Styrene butadiene rubber (SBR)	20	20	20	20	20
Rice husk powder (RHP)	0	15	30	45	60

^a php, part per hundred polymer.

200°C. Styrene butadiene rubber (SBR) (Buna huls, 1502) was obtained from Bayer AG (Leverkusen, Germany). The rice husk powder (particle size 1.23–8.30 μm) was obtained from Bernas Perdana Sdn. Bhd. (Penang, Malaysia). Maleic anhydride (MA) was obtained from Fluka Chemical (Buchs, Switzerland) with 99% purity, xylene from Merck (Darmstadt, Germany), acetic acid from J.T. Baker Inc., and MA-PP from Aldrich Chemical Co. (Milwaukee, WI), with MFI value of 11.5 g/10 min.

Mixing procedure

The mixing of composite was carried out in a Brabender Plasticoder model PLE 331 (Brabender Instruments, South Hackensack, NJ) at a temperature of 170°C and a rotor speed of 50 rpm for 10 min. The polystyrene was preheated for 2 min before the rotor started and was melted in the mixer for 2 min. Then RHP was added to the molten PS and the mixing was continued for another 2 min. SBR was added as a last component and was mixed for an additional 4 min. Table I shows the composition of the composite. For composites with coupling agent, 2% (by filler weight) of MA-PP was added in the molten PS during the 3rd min. A torque versus time curve was also plotted for each composition during the mixing process to monitor the processing condition. The composites were then press heated to produce molded sheets (1 and 3 mm thick) for use in tensile and impact tests, respectively.

Esterification

The fiber was first dried at 105°C overnight before use. The RHP was esterified by using 2% MA in xylene, keeping the fiber to solvent ratio at 1:20 (w/v). The RHP was soaked in MA for 18 h at 65°C. The RHP was filtered out and dried in an oven.

Acetylation

The fiber was first dried at 105°C overnight before use. The RHP was soaked in a 50% acetic acid aqueous solution and stirred for 1 h, with filler to solution ratio

at 1:25. Then the RHP was filtered out, washed, and dried in an oven.

Tensile properties

Tensile properties were tested with a Tensometric tensometer M 500 (Lancashire, UK), according to ASTM D412, at a crosshead speed of 50 mm/min. The press-heated molded samples (1 mm thick) were cut into dumbbell shape using a Wallace die cutter. A minimum of five samples was tested in each series.

Impact test

The Izod impact strength was measured using a Zwick testing machine operating with a 7.5 J pendulum according to ASTM D256. The press-heated molded samples (3 mm thick) were cut into bar shape (50 mm width \times 170 mm length). A minimum of five samples was tested in each series.

Ageing studies

Tensile samples underwent thermooxidative ageing, conducted in an air-circulating oven, operating at 70°C for 7 days. After being cooled and conditioned at room temperature in the desiccators, the dimensions of each specimen were measured. The tensile properties of these samples as a function of ageing were determined using the procedures mentioned above.

Water absorption test

The tensile specimens of 1 mm thickness were used to study the water absorption. The samples were immersed in distilled water and the percentage weight change was determined until the equilibrium value was reached. After immersion in distilled water, specimens were removed at different times, wiped with tissue paper to remove excess water, and weighed with an analytical balance with 0.1 mg resolution. The percentage of weight gain was then calculated as follows:

$$W_t = \frac{W_t - W_0}{W_0} \times 100\% \quad (1)$$

where W_t is the percentage of weight gain, W_0 is the weight of the dry sample, and W_t is the weight of the wet sample. A minimum of five samples was tested in each series.

Morphology study

Examination of the tensile fracture surfaces was performed using a scanning electron microscope (SEM);

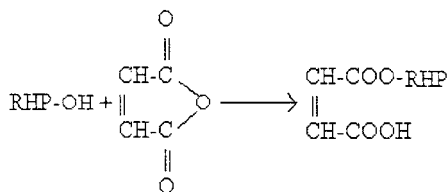


Figure 1 Reaction formula for RHP reacted with maleic anhydride for esterification.

model Leica Cambridge S-360; Wetzlar, Germany). All the fracture surfaces of selected samples were examined after first sputter coating with gold to avoid electrostatic charging and poor image resolution.

FTIR analysis

FTIR spectra were obtained using an FTIR Model PE 4000 series (Perkin Elmer Cetus Instruments, Norwalk, CT) apparatus. The spectra resolution was set at 4 cm^{-1} and the scanning range was set from 600 to 4000 cm^{-1} . The rice husk powder was dispersed in potassium bromide (KBr) to obtain the required discs. Both RHP and KBr were carefully dried before disk preparation and immediately used for FTIR analysis.

RESULTS AND DISCUSSION

FTIR analysis

The test was conducted on RHP, which was subjected to chemical treatment to determine the existence of functional group in the filler before and after the treatment. Figures 1 and 2 show the hypothesis of reaction formula during esterification and acetylation process of RHP. Figures 3–5 show FTIR spectra for untreated, acetylated, and esterified RHP, respectively. Because the RHP is a highly hydrophilic component, the slight reduction in the intensity of -OH stretching absorption band at around 3390 cm^{-1} might be attributable to the effect of moisture. For the acetylation treatment, the intensity at 1726.6 cm^{-1} indicates the existence of an acetyl group (CH_3CO). The success of the esterification reaction was demonstrated by FTIR spectra (Fig. 5). The peak at 1726 cm^{-1} (C=O) indicated the presence of an ester group and the intensity at 1647 cm^{-1} appeared because of the double bond of the introduced propenoic acid side chain (-CO-CH=CH-COOH). The peak at 1650 cm^{-1} in untreated and acetylated fillers is attributed to the C=C stretching from the hemicellulose component, which was partially removed after esterified treatment, indicating that the hemicellulose in the fibers is easily removed by esterification.

Torque development

Figures 6 and 7 show the effect of chemical treatment and coupling agent (MA-PP) on torque-time curves for RHP/PS-SBR composites using 15 parts per hundred polymer (php) and 45 php of RHP. In general, all torque-time curves for each composition have a similar pattern of three upward peaks and one downward peak. Three upward peaks represent PS loading, RHP loading and SBR loading, respectively. These peaks start to decrease when PS undergoes fusion, RHP disperses in molten PS, and SBR become soft as the mixing time increases. The downward peak at the 4th min occurs because of the instant lubricant action from the fine RHP particle.¹ The torque values stabilize at the end of mixing time (10th min), which indicates that the mixing process was completed. For composites with coupling agent, MA-PP was added in molten PS at the 3rd min.

Stabilization torque at the end of the mixing process versus filler loading for untreated, chemically treated composites, and composites with MA-PP are shown in Figure 8. As can be seen, the stabilization torque increases with an increase in RHP loading for all types of treatment. MA-PP and acetylated composites have a stabilization torque value similar to that of untreated composites. MA-PP-modified composites show a decrease in torque value during processing compared to untreated composites, although the stabilization torque shows no evidence of a significant reduction because it is believed that the MA-PP enhances the interaction between filler and matrix, which thus increased the torque value at the end of processing time. However, esterified composites have a lower stabilization torque compared to that of other composites, which is attributed to the lubricant action from the MA component in the RHP/PS-SBR composites, thus reducing the torque value during the mixing of the composites. Marcovich et al.⁷ reported that MA acts as a coating layer and is evenly distributed onto the surface, causing the plasticization and lubricant action on the filler.

Mechanical properties

Figures 9–12 show the effect of chemical treatment and coupling agent on the mechanical properties of RHP/PS-SBR composites at different filler loadings.

Tensile strength

The tensile strength of RHP/PS-SBR composites is demonstrated in Figure 9. In general, the tensile



Figure 2 Reaction formula for RHP reacted with acetic acid for acetylation.

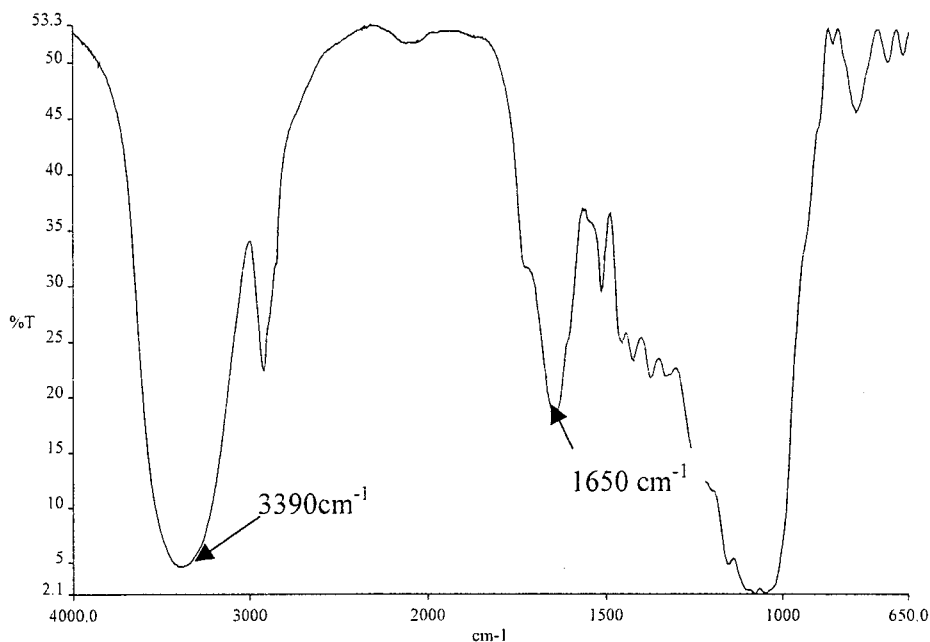


Figure 3 Infrared spectra of untreated RHP.

strength decreases with increased RHP loading. Incorporation of filler in the polymer matrix will reduce the ability of the composites to transfer applied stress, especially particulate filler of irregular shape. Our previous work¹ showed that RHP consists of irregularly shaped filler. Results show that the tensile strength decreased by the order of MA-PP > untreated > acetylated > esterified composites. This indicates that the MA-PP in the RHP/PS-SBR composites improved the interaction between filler and matrix, causing a more effective transfer of the stresses from ma-

trix to filler, thus increasing the tensile strength of the composites. Oksman and Clemons⁸ found that MA-PP improved the interfacial adhesion between PP and wood flour and increased the tensile strength of the composites. Ichazo et al.⁴ also reported similar findings in their research on PP/wood flour composites.

Acetylated composites have tensile strength that is almost identical to that of untreated composites. Analysis of SEM micrographs (see next section) shows that there is good interaction between filler and matrix in these composites. However, the existence of filler ag-

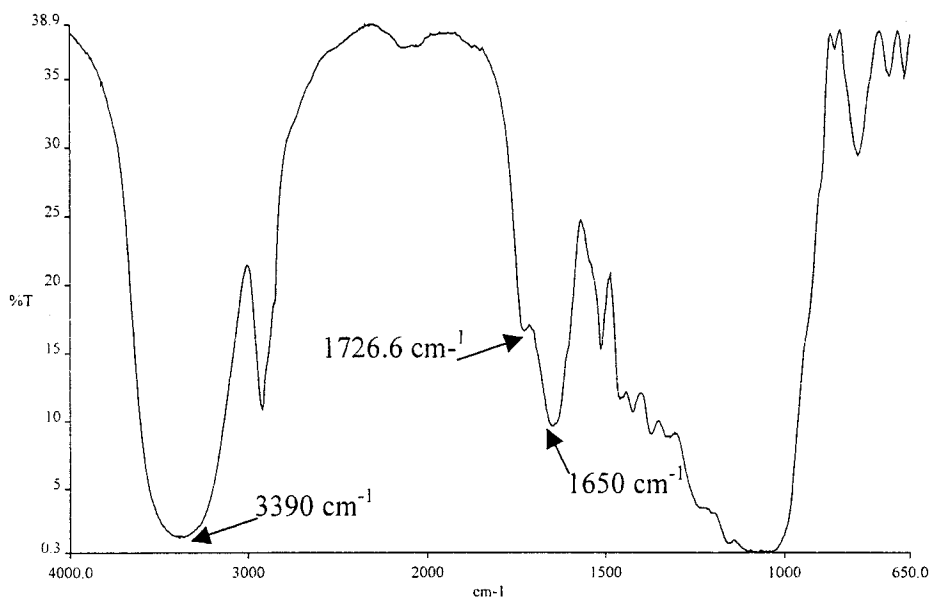


Figure 4 Infrared spectra of acetylated RHP.

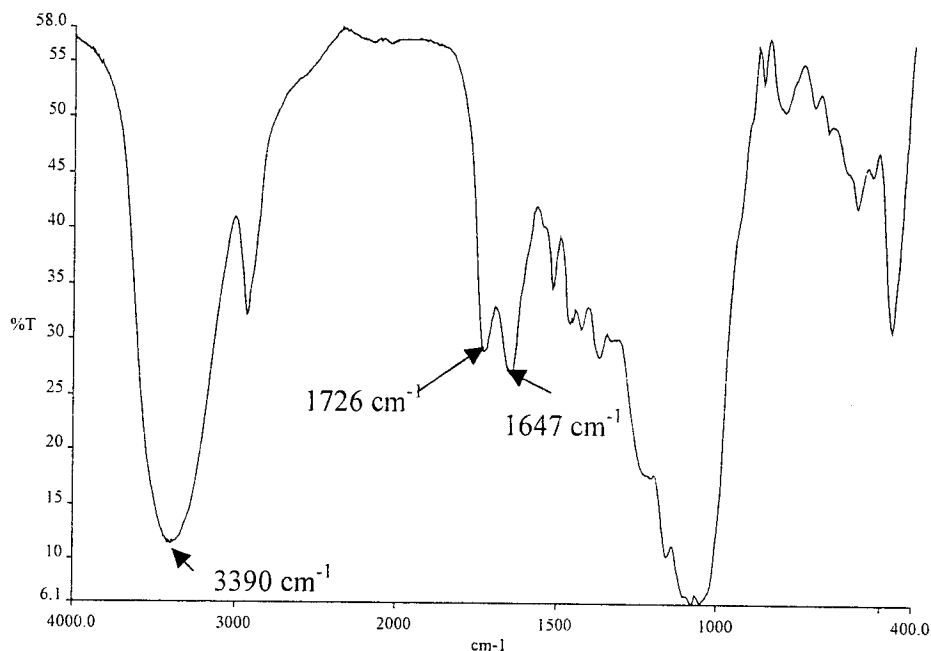


Figure 5 Infrared spectra of esterified RHP.

glomerates is believed to reduce the tensile strength of acetylated composites because the filler agglomerates can act as a stress concentration point, thus increasing the ability of the composites to initiate matrix cracks. For esterified composites, lubricant actions from maleic anhydride reduced its tensile strength. At 15 php of filler loading, most of the composites show higher tensile strength, except for esterified composites. As reported by Ismail et al.,¹ RHP acts as a reinforcing material at this loading.

Elongation at break

Figure 10 shows the elongation at break as a function of filler loading for RHP/PS-SBR composites with chemical treatment and MA-PP. In general, elongation at break decreases for all types of treatment compared to that in untreated composites, decreasing in the order of untreated > acetylated > MA-PP > esterified composites.

The waxy substances (lignin and hemicellulose) of natural fillers, which can be eliminated with chemical

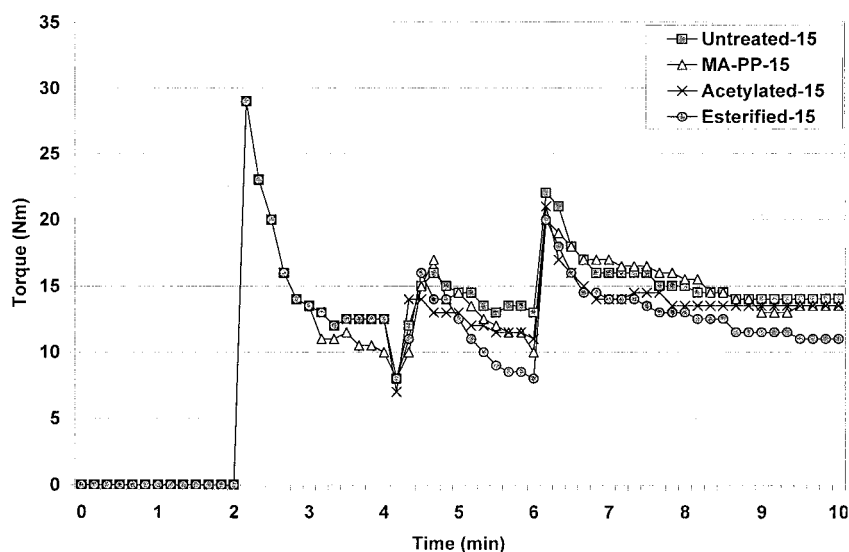


Figure 6 Brabender torque-time curves for PS/SBR/RHP composites with chemical treatment and coupling agent at 15 php filler loading.

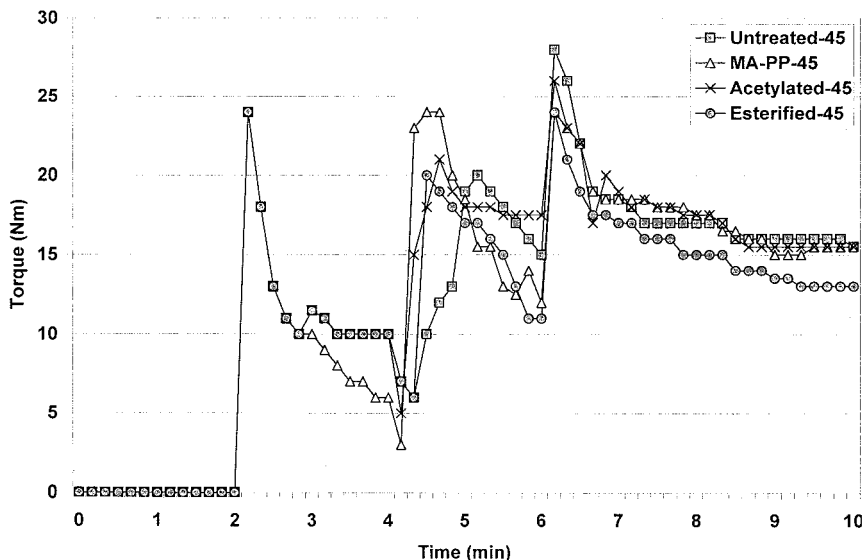


Figure 7 Brabender torque–time curves for PS/SBR/RHP composites with chemical treatment and coupling agent at 45 php filler loading.

treatment, are the cause of the fillers’ wettability and adhesion between filler and polymer matrix.⁹ Without the waxy substance, the fillers’ wettability and adhesion with matrix decrease, thus causing a reduction in elongation at break. FTIR analysis shows that the waxy components diminished after esterification treatment and were partially removed during the acetylation treatment, which provides evidence of higher elongation at break for acetylated composites than that for esterified composites. For MA-PP composites, elongation at break decreases because of improved interaction between filler and matrix in RHP/PS-SBR composites. Ichazo et al.⁴ and Meyers et al.¹⁰ reported similar findings where MA-PP reduced the elongation at break for PP/wood flour composites.

Young’s modulus

Young’s modulus for RHP/PS-SBR composites at different filler loadings with chemical treatment and MA-PP is demonstrated in Figure 11. As can be seen, composites with chemical treatment and MA-PP produce lower Young’s modulus compared to that of untreated composites, particularly at filler loadings, > 15 php. Rong et al.¹¹ found that chemical treatment induced a lower modulus value because of changes in the cell structure of natural fillers, where the swelling of cellulose and part of lignin and hemicellulose have been removed. He also reported that sisal fibers become ductile after the removal of lignin and hemicellulose. There is no

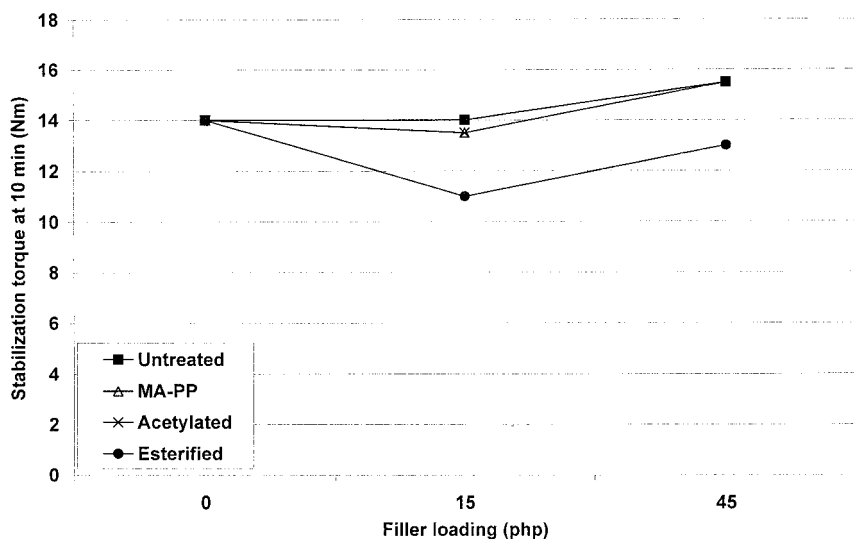


Figure 8 Equilibrium torque at 10 min for PS/SBR/RHP composites with chemical treatment and coupling agent.

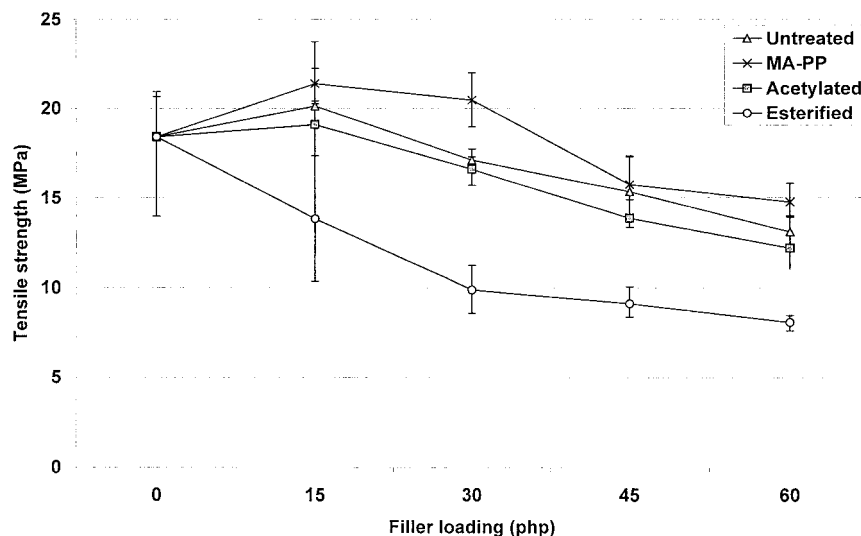


Figure 9 Effect of filler loading on the tensile strength of PS/SBR/RHP composites with chemical treatment and coupling agent.

significant change in Young's modulus with the increase in filler loading except for untreated composites. For MA-PP composites, Young's modulus decreases as a result of lubricant action from the component of maleic anhydride in the composites. The stabilizing torque versus time curve (Fig. 8) shows the obvious lubrication action of the esterified composites, thus proving that the lubrication effect can reduce the stiffness of the esterified composites. This result provides evidence that the stiffness of the RHP/PS-SBR composites decreases with the introduction of chemical treatment and the use of MA-PP.

Impact strength

Figure 12 shows the impact strength of RHP/PS-SBR composites with chemical treatment and MA-PP at different filler loadings. As can be seen in the figure, impact strength decreases with the increase in filler loading. This is because the filler cannot resist crack propagation as effectively as can the polymer region, thus causing a reduction in impact strength with the increase in filler loading. RHP/PS-SBR composites with MA-PP have a higher impact strength compared to that of others. This is attributed to improved interaction between

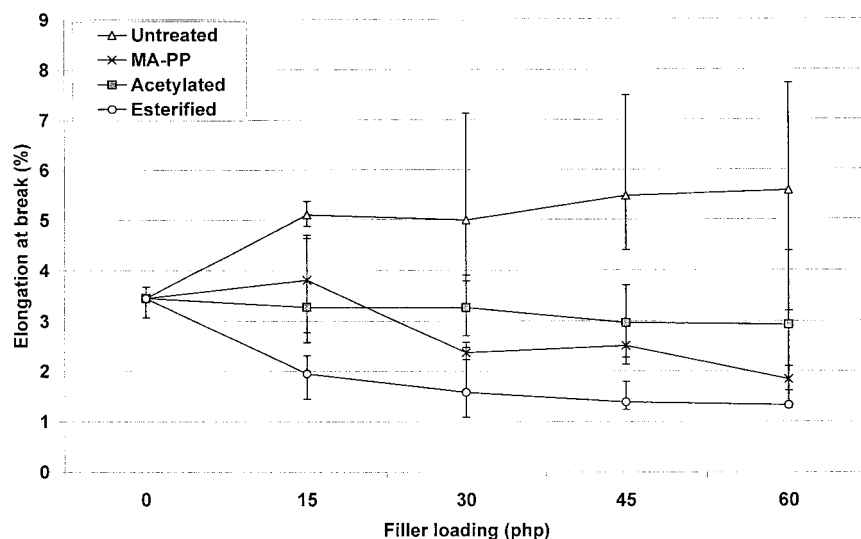


Figure 10 Effect of filler loading on the elongation at break of PS/SBR/RHP composites with chemical treatment and coupling agent.

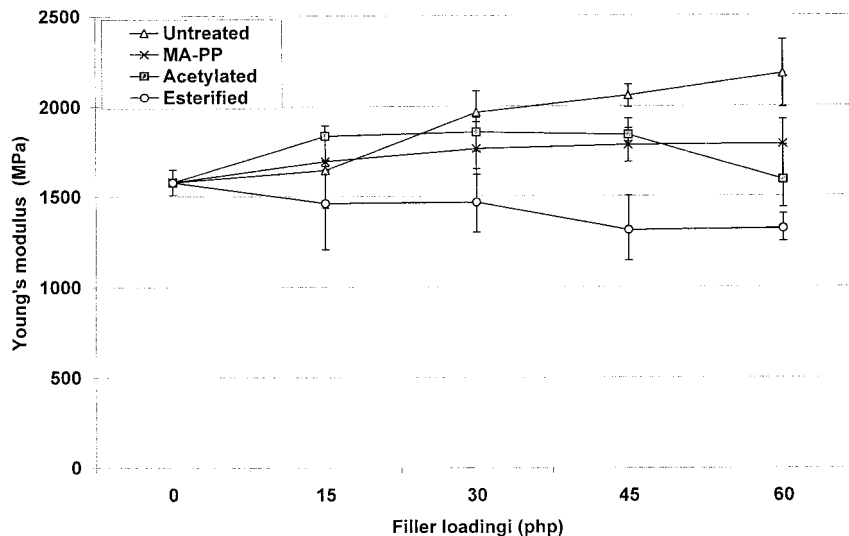


Figure 11 Effect of filler loading on the Young modulus of PS/SBR/RHP composites with chemical treatment and coupling agent.

the filler and matrices in these composites, which thus enhances the effectiveness of stress transfer during the impact test and produces higher impact strength. Lubricant actions in the esterified composites also have the ability to improve the resistance toward the impact test. Higher impact strength in acetylated composites, compared to that of untreated composite, indicates that there is an interaction between filler and matrix in this composite.

Effect of thermooxidative ageing on the tensile properties of the composites

Figures 13–15 show the tensile strength, elongation at break, and Young’s modulus for RHP/PS–SBR

composites with chemical treatment and MA–PP at different filler loadings before and after the ageing test. Results showed that the tensile strength increases after the ageing test for MA–PP and esterified composites (Fig. 13). This might be attributable to the postreaction process of the composite materials. Maleic anhydride is an active substance that can react or be grafted with polymer radicals.^{12,13} It is believed that during the ageing process, scissions of polystyrene and styrene butadiene rubber chain took place, which produced their radicals.¹⁴ The excess maleic anhydride on the filler surface tends to react with these polymer radicals and become grafted to each other.¹⁵ This phenomenon will increase the crosslinking between filler and matrices,

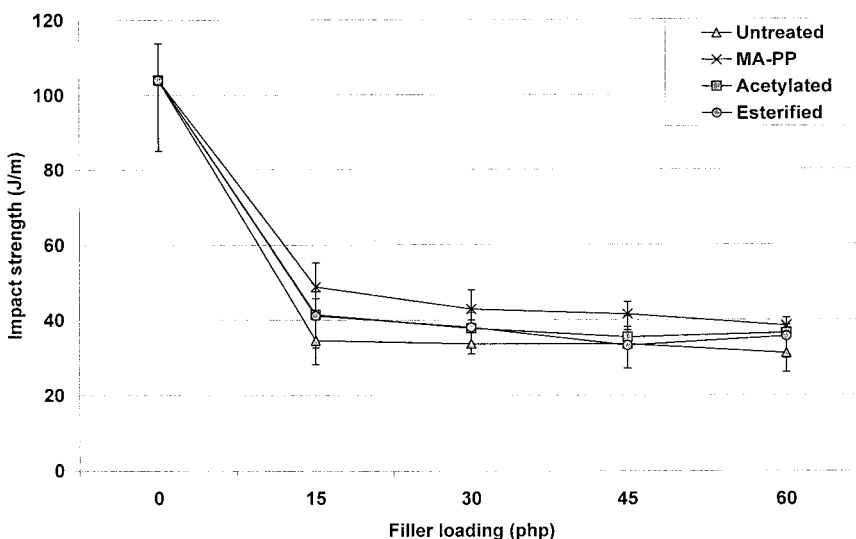


Figure 12 Effect of filler loading on the impact strength of PS/SBR/RHP composites with chemical treatment and coupling agent.

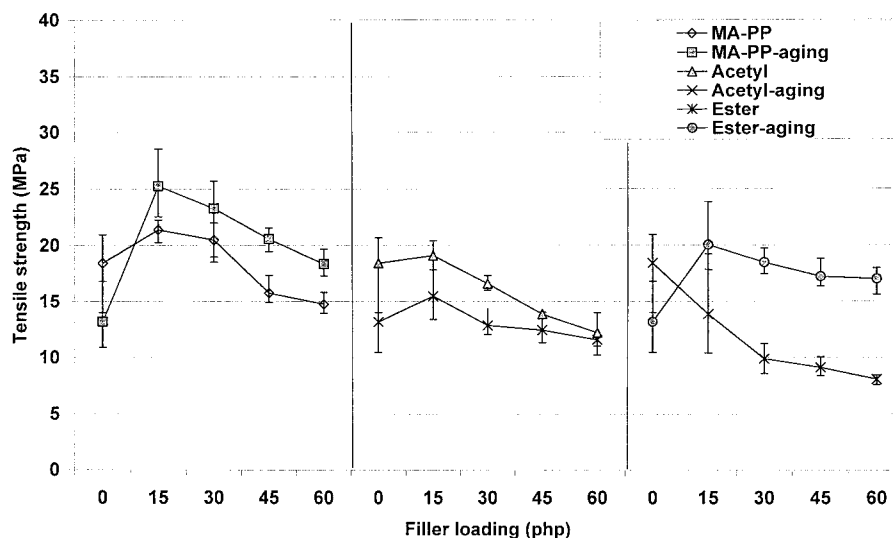


Figure 13 Effect of thermooxidative ageing (at 70°C for 7 days) on tensile strength of PS/SBR/RHP composites with chemical treatment and coupling agent.

thus enhancing the tensile strength. For acetylated composites, the tensile strength decreases after the ageing test for all compositions. This might be attributable to the degradation of the PS and SBR chain during the ageing test.

Elongation at break (Fig. 14) decreases after the ageing test for all samples, where the composites change to a stiffer material. Increased interaction between filler and matrix after the ageing test for MA-PP and esterified composites also reduces the elongation at break. Figure 15 shows the Young's modulus for all samples after the ageing test. In general, an increase in Young's modulus indicates that the stiffness of all samples increases after the ageing test.

Water absorption

Figure 16 shows the percentage of water absorption in RHP/PS-SBR composites with loading and MA-PP at different filler loading. As can be seen, the percentage of water absorption increases with the increase in filler loading because of the increase in polarity of the composites with the increase in the polar component (RHP). Acetylated composites show a lower percentage of water absorption, which indicates that acetyl groups that had substituted the hydrogen atoms of the hydroxyl groups in RHP have reduced the hygroscopicity of the filler. Chang and Chang³ reported that the acetyl group, which has a greater molecular volume, occupied more space in the

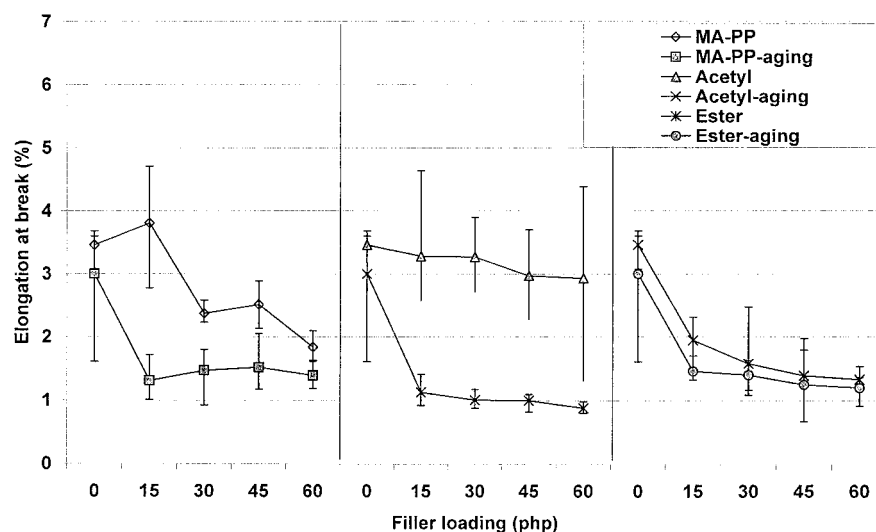


Figure 14 Effect of thermooxidative ageing (at 70°C for 7 days) on elongation at break of PS/SBR/RHP composites with chemical treatment and coupling agent.

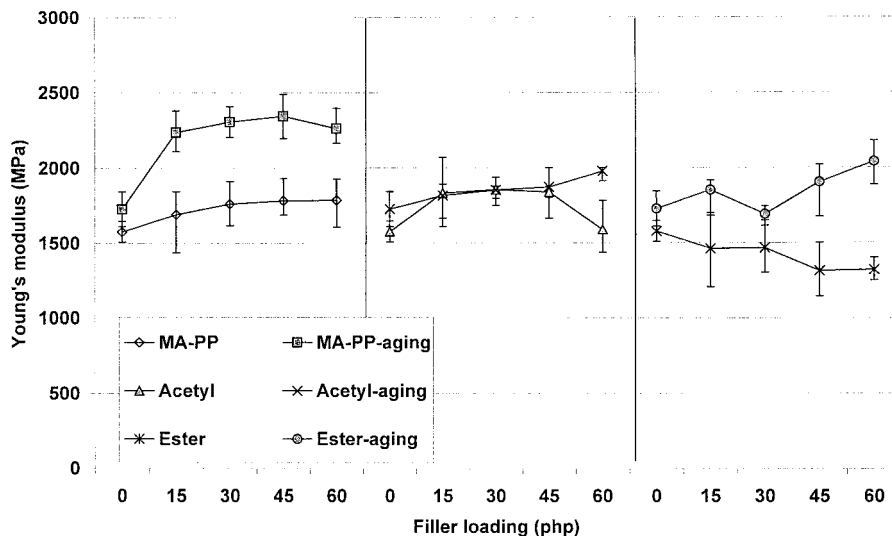


Figure 15 Effect of thermooxidative ageing (at 70°C for 7 days) on Young modulus of PS/SBR/RHP composites with chemical treatment and coupling agent.

cell wall and thus reduced the moisture to the sorption sites. Esterified composites and composites with MA-PP show a slightly lower percentage of water absorption compared to that of untreated composites, which is attributed to less interaction and adhesion between filler and matrices in esterified composites; besides, MA-PP does not fully react with hydroxyl groups in RHP. Thwe and Liao^{16,17} reported that MA-PP in bamboo fiber/PP composites has a reduced percentage of water absorption. The reduction in moisture level is believed to be attributable to the improved interfacial adhesion that reduces water accumulation in the interfacial voids and prevents water from entering the bamboo fiber.

Acetylation treatment is effective in reducing the percentage of water absorption in RHP/PS-SBR composites. Figure 17 shows the equilibrium of water absorption in all samples. As can be seen, acetylated composites have a lower equilibrium value than that of other composites.

Morphology

SEM micrographs in Figures 18–24 show the tensile fractured surface of the composites with chemical treatment and MA-PP at two different filler loadings (15 and 60 ph). In general, there are more filler agglomerates in RHP/PS-SBR composites at the

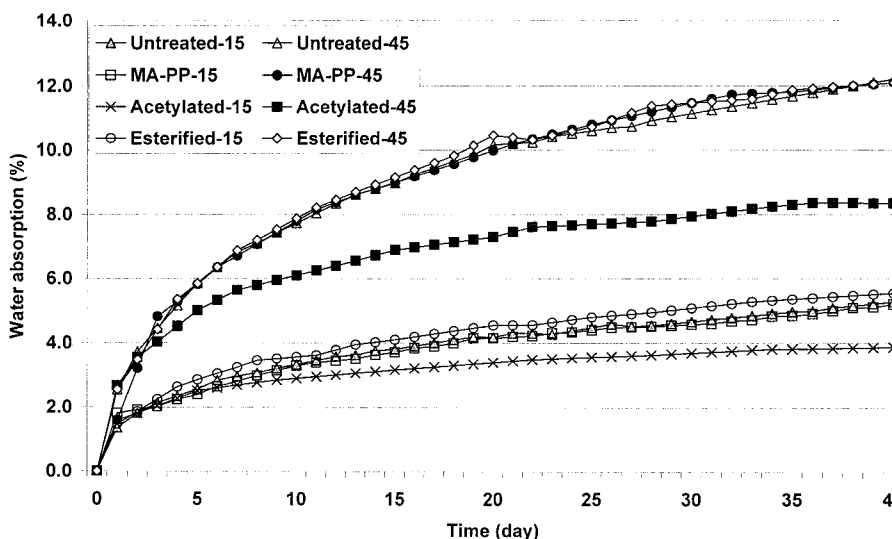


Figure 16 Absorption of water at ambient temperature in PS/SBR/RHP composites with chemical treatment and coupling agent.

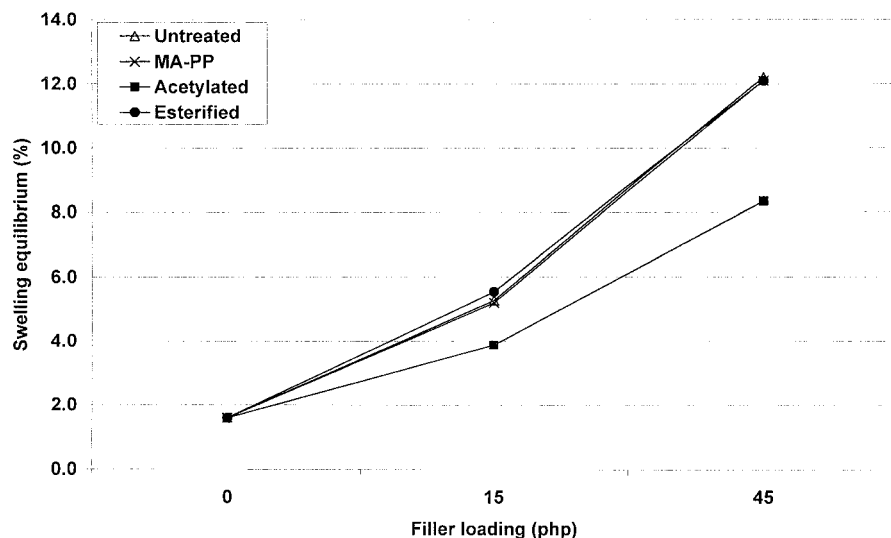


Figure 17 Equilibrium swelling at 40 days immersion in water for PS/SBR/RHP composites with chemical treatment and coupling agent.

higher filler loading, 60 php (Fig. 20, 22, and 24). This phenomenon will cause the reduction in tensile strength and Young's modulus of the composites at higher filler loading. Composites with MA-PP at 15 php RHP loading (Fig. 19) exhibit a smooth fractured surface, with fillers embedded in the matrix and fully covered by the matrix with no sign of air trapped in the composites, compared to untreated composites (Fig. 18). This indicates that MA-PP improves the interfacial adhesion between matrix and filler, thus increasing the tensile strength of the composites.

For esterified composites at 15 php RHP loading (Fig. 21), the SEM micrograph shows matrix tearing, which is attributed to the effect of lubricant action

induced by the maleic anhydride component, which caused the composites to become softer and to have a lower tensile strength.

Acetylated composites at 15 php RHP loading (Fig. 23) exhibit smooth and uniform fractured surfaces that indicate better interfacial adhesion between filler and matrix. However, the existence of filler agglomerates in this composite reduced the tensile strength. In general, RHP/PS-SBR composites with chemical treatment and MA-PP produce a better matrix phase and filler distribution, although the degree of filler-matrix interaction was primarily responsible for the improvement of mechanical properties in the composites.

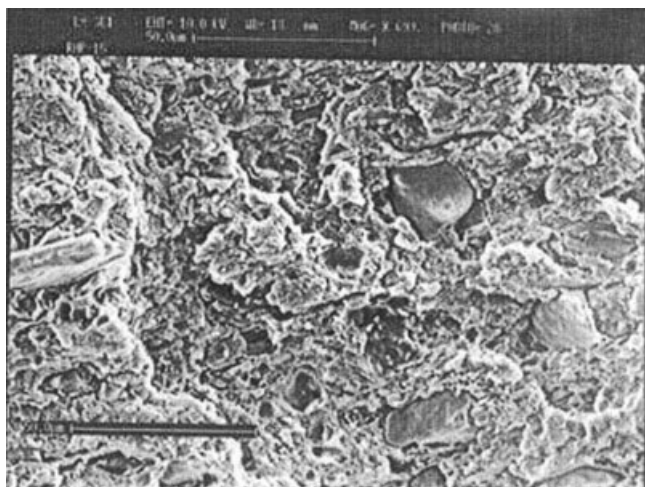


Figure 18 Scanning electron micrograph of tensile fracture surface of untreated RHP/PS/SBR composite (15 php) at magnification of $\times 700$.

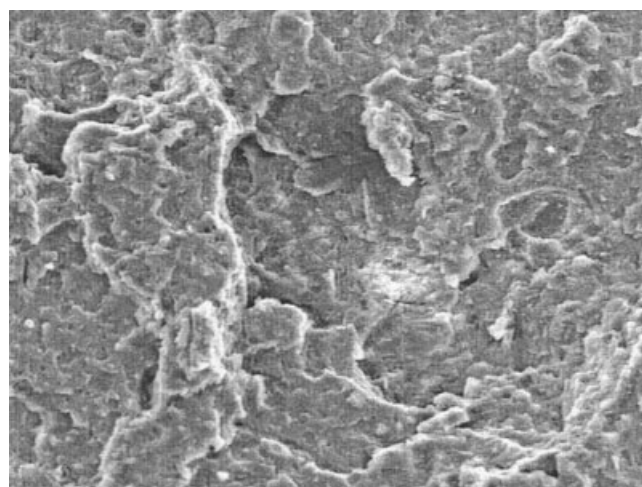


Figure 19 Scanning electron micrograph of tensile fracture surface of RHP/PS/SBR composite (15 php) with MA-PP at magnification of $\times 700$.

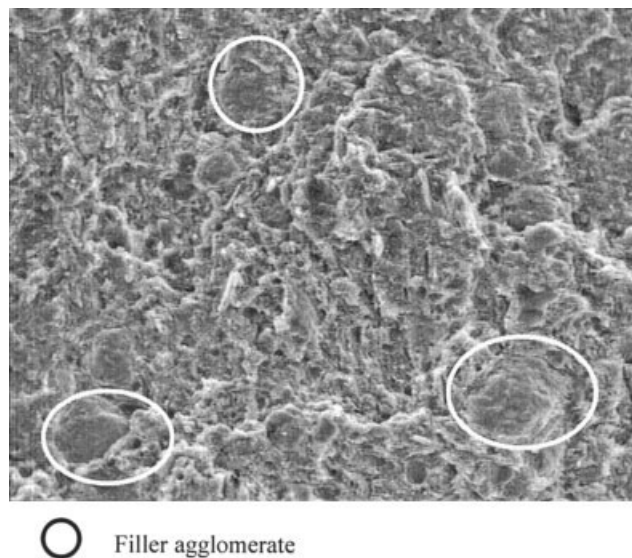


Figure 20 Scanning electron micrograph of tensile fracture surface of RHP/PS/SBR composite (60 php) with MA-PP at magnification of $\times 700$.

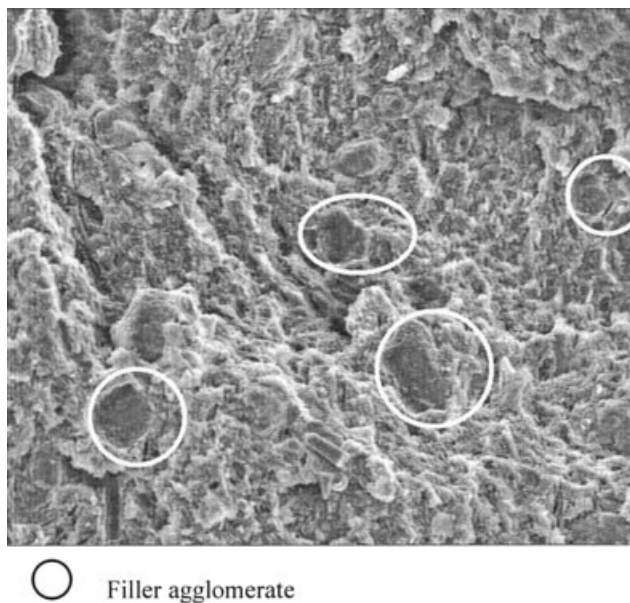


Figure 22 Scanning electron micrograph of tensile fracture surface of esterified RHP/PS/SBR composite (60 php) at magnification of $\times 700$.

CONCLUSIONS

Based on the above results and discussion, the following statements can be drawn:

1. The MA-PP composites improve the mechanical properties and the dispersion of the filler compared to untreated composites.
2. The esterified composites improve only the dispersion of the filler, but not their adhesion to the polymer matrix, as indicated by tensile properties and SEM analysis.
3. Ageing of esterified and MA-PP composites enhanced the tensile strength and Young's

modulus of the composites as a result of the postreaction process during the ageing test.

4. RHP/PS-SBR composites with chemical treatment and MA-PP produce a better matrix phase and filler distribution, although the degree of filler-matrix interaction was chiefly responsible for the improvement of mechanical properties in the composites.
5. Acetylation treatment is effective in reducing the percentage of water absorption in RHP/

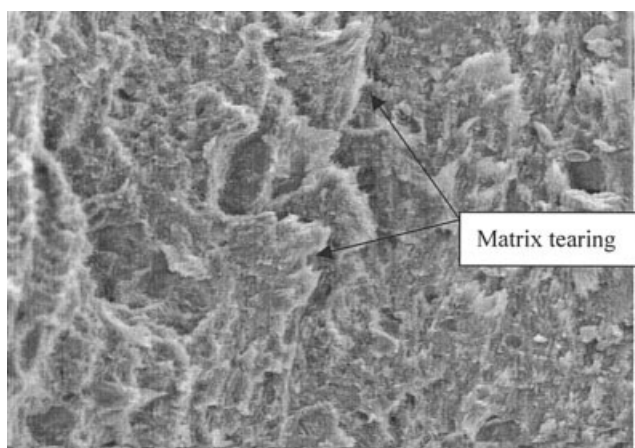


Figure 21 Scanning electron micrograph of tensile fracture surface of esterified RHP/PS/SBR composite (15 php) at magnification of $\times 700$.

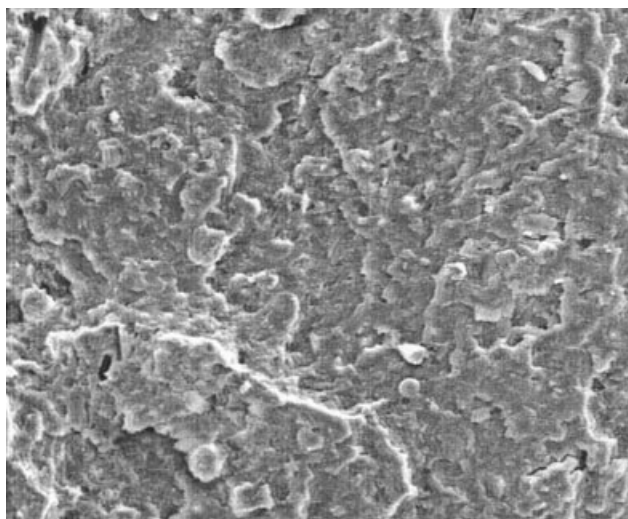
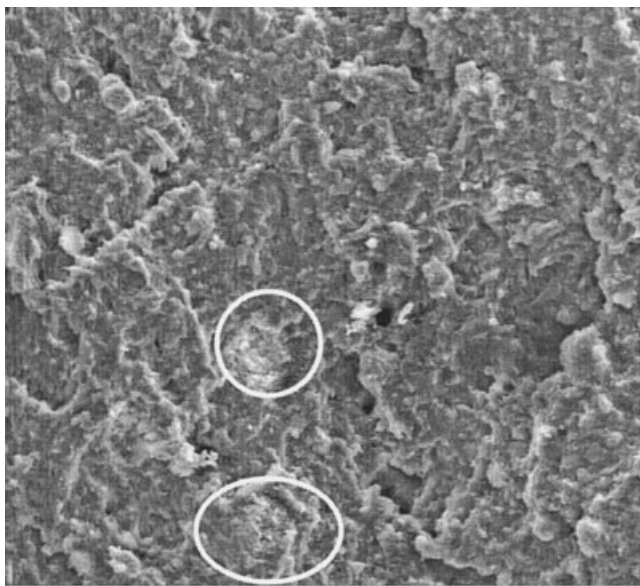


Figure 23 Scanning electron micrograph of tensile fracture surface of acetylated RHP/PS/SBR composite (15 php) at magnification of $\times 700$.



○ Filler agglomerate

Figure 24 Scanning electron micrograph of tensile fracture surface of acetylated RHP/PS/SBR composite (60 php) at magnification of $\times 700$.

PS-SBR composites where acetyl groups, which substituted the hydrogen atoms of the hydroxyl groups in RHP, reduced the hygroscopicity of the RHP.

References

1. Ismail, H.; Mohamad, Z.; Bakar, A. A. *Polym Plast Technol Eng* 2003, 42, 81.
2. Hottotuwa, G. B.; Ismail, H.; Azahari, B. *Polym Test* 2002, 21, 833.
3. Chang, S. T.; Chang, H. T. *Polym Degrad Stab* 2001, 71, 261.
4. Ichazo, M. N.; Albano, C.; Gonzalez, J.; Perera, R.; Candal, M. V. *Comp Struct* 2001, 54, 207.
5. Bajardo, M.; Frisoni, G.; Scandola, M.; Licciardello, A. *J Appl Polym Sci* 2002, 83, 38.
6. Mwaikambo, L. Y.; Ansell, M. P. *J Appl Polym Sci* 2002, 84, 2222.
7. Marcovich, N. E.; Aranguren, M. I.; Reboredo, M. M. *Polymer* 2001, 42, 815.
8. Oksman, K.; Clemons, C. *J Appl Polym Sci* 1998, 67, 1503.
9. Bledzki, A. K.; Reihmane, S.; Gassan, J. *J Appl Polym Sci* 1996, 59, 1329.
10. Meyers, G. E.; Chahyadi, I. S.; Coberly, C. A.; Ermer, D. S. *Int J Polym Mater* 1991, 15, 21.
11. Rong, M. Z.; Zhang, M. Q.; Liu, Y.; Yang, G. C.; Zeng, H. M. *Compos Sci Technol* 2001, 61, 1437.
12. Joseph, S.; Oommen, Z.; Thomas, S. *Mater Lett* 2002, 53, 268.
13. Dalvag, H.; Klason, C.; Stromvall, H. E. *Int J Polym Mater* 1985, 11, 9.
14. Shelton, J. R. In: *Concise Encyclopedia of Polymer Processing and Application*; Corish, P. J., Ed.; Pergamon: New York, 1991.
15. Rozman, H. D.; Saad, M. J.; Mohd Ishak, Z. A. *Polym Test* 2003, 22, 335.
16. Thwe, M. M.; Liao, K. *Compos Part A: Appl Sci Manuf* 2002, 33, 43.
17. Thwe, M. M.; Liao, K. *Compos Sci Technol* 2003, 63, 375.